



# Spatiotemporal Changes of Near-Surface Ozone Concentration From 2015 to 2018 in Beijing

Junfei Xie<sup>1</sup>, Shengwei Shi<sup>2</sup>, Lingyun Wu<sup>3\*</sup> and Xin Zhang<sup>4</sup>

<sup>1</sup>Beijing Key Laboratory of Ecological Function Assessment and Regulation Technology of Green Space, Beijing Institute of Landscape Architecture, Beijing, China, <sup>2</sup>College of Bioscience and Resources Environment, Beijing University of Agriculture, Beijing, China, <sup>3</sup>State Key Laboratory of Numerical Modeling for Atmospheric Sciences and Geophysical Fluid Dynamics (LASG), Institute of Atmospheric Physics, Chinese Academy of Sciences, Beijing, China, <sup>4</sup>College of Landscape Architecture and Tourism, Hebei Agricultural University, Hebei, China

## OPEN ACCESS

### Edited by:

Gert-Jan Steeneveld,  
Wageningen University and Research,  
Netherlands

### Reviewed by:

Maria De Fatima Andrade,  
University of São Paulo, Brazil  
Despina Georgios Deligiorgi,  
National and Kapodistrian University of  
Athens, Greece

### \*Correspondence:

Lingyun Wu  
wuly@lasg.iap.ac.cn

### Specialty section:

This article was submitted to  
Atmospheric Science,  
a section of the journal  
Frontiers in Environmental Science

**Received:** 19 August 2020

**Accepted:** 26 April 2021

**Published:** 11 May 2021

### Citation:

Xie J, Shi S, Wu L and Zhang X (2021)  
Spatiotemporal Changes of Near-  
Surface Ozone Concentration From  
2015 to 2018 in Beijing.  
*Front. Environ. Sci.* 9:593220.  
doi: 10.3389/fenvs.2021.593220

In this study, we investigated the spatiotemporal changes of near-surface O<sub>3</sub> concentration based on 33 automatic air quality monitoring stations in Beijing in 2015 and 2018. Here we show that the diurnal variations for O<sub>3</sub> concentration at 33 monitoring stations exhibited a single-peak mode with a minimum concentration from 06:00 to 07:00 and a maximum value from 14:00 to 15:00. We find that the O<sub>3</sub> concentration was significantly positively correlated with the air temperature, solar total radiation, and wind speed, while it was negatively correlated with the relative humidity. Among those factors, the air temperature played the most important role in influencing O<sub>3</sub> concentration (relative contribution is greater than 88% in the boosted regression trees model). We also present that the annual variation of O<sub>3</sub> concentration at all stations tended to be a “bell-shaped” curve distribution with a peak in summer and the lowest value in winter. The annual averaged O<sub>3</sub> concentration at 33 stations in Beijing was 57.5 ± 9.8 μg·m<sup>-3</sup> in 2015 and 60.3 ± 9.0 μg·m<sup>-3</sup> in 2018. In addition, we detect that the annual averaged value of the O<sub>3</sub> concentration was lower in the central and southern Beijing, and higher in the northern Beijing both in 2015 and 2018. The spatial difference of the O<sub>3</sub> concentration could be explained by the traffic pollution, vegetation coverage, atmospheric regional transmission, and atmospheric particulate matter concentration.

**Keywords:** surface ozone concentration, spatiotemporal change, boosted regression trees model, urban environment, Beijing

## INTRODUCTION

Although the stratospheric ozone (O<sub>3</sub>) layer can absorb ultraviolet light and protect the Earth's biosphere, the O<sub>3</sub> in the troposphere, especially near the ground, is an air pollutant. As a strong oxidizing gas, O<sub>3</sub> can rapidly and heterogeneously react with organic matter in biological systems (Lehman et al., 2004; Wang et al., 2015). High O<sub>3</sub> concentrations can affect human health Kong et al. (1999), Raddatz and Cummie (2001), Wang et al. (2017), cause damage to plant leaves, and trigger the synthetic release of plant volatile organic compounds (VOCs) (Velikova et al., 2005; Calfapietra et al., 2008; Loreto and Schnitzler, 2010; Yuan et al., 2017).

Ozone is a secondary pollutant, therefore, its formation is complex. The precursor of ozone formation is a key factor. Investigations show that volatile organic compounds (VOCs) and nitrogen

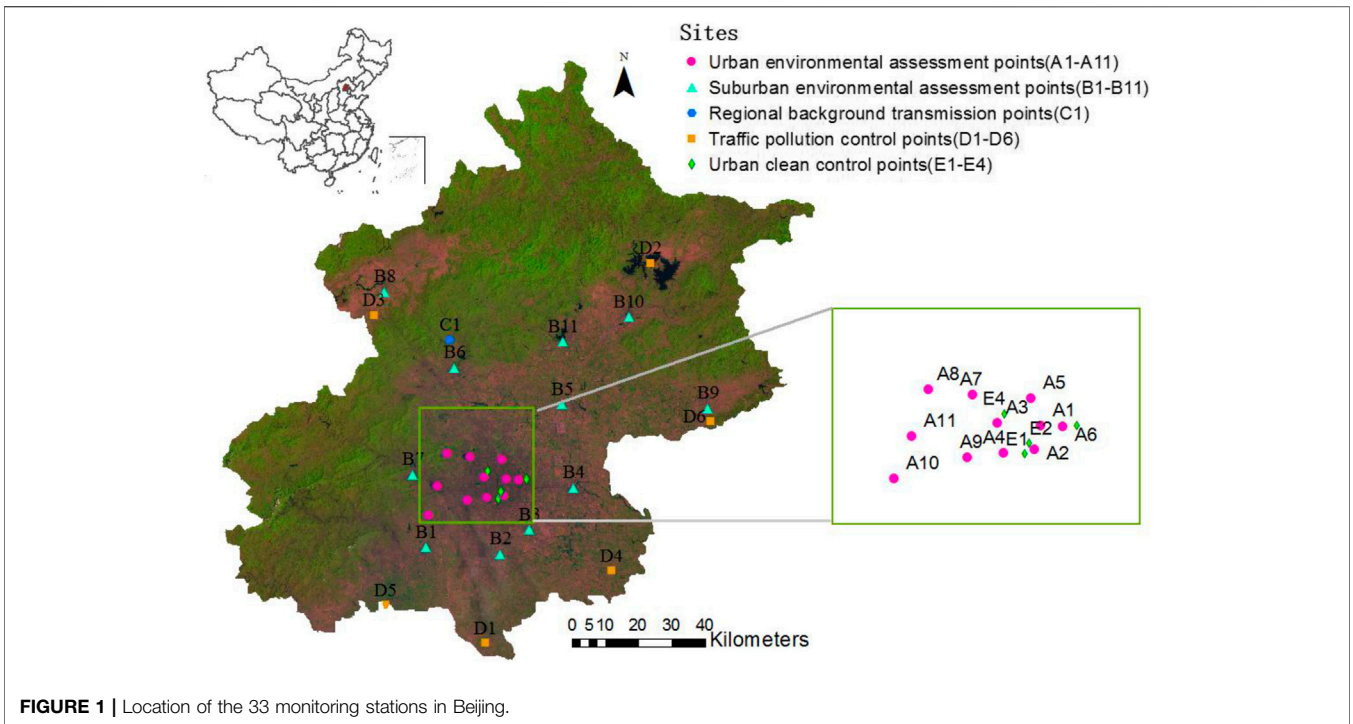


FIGURE 1 | Location of the 33 monitoring stations in Beijing.

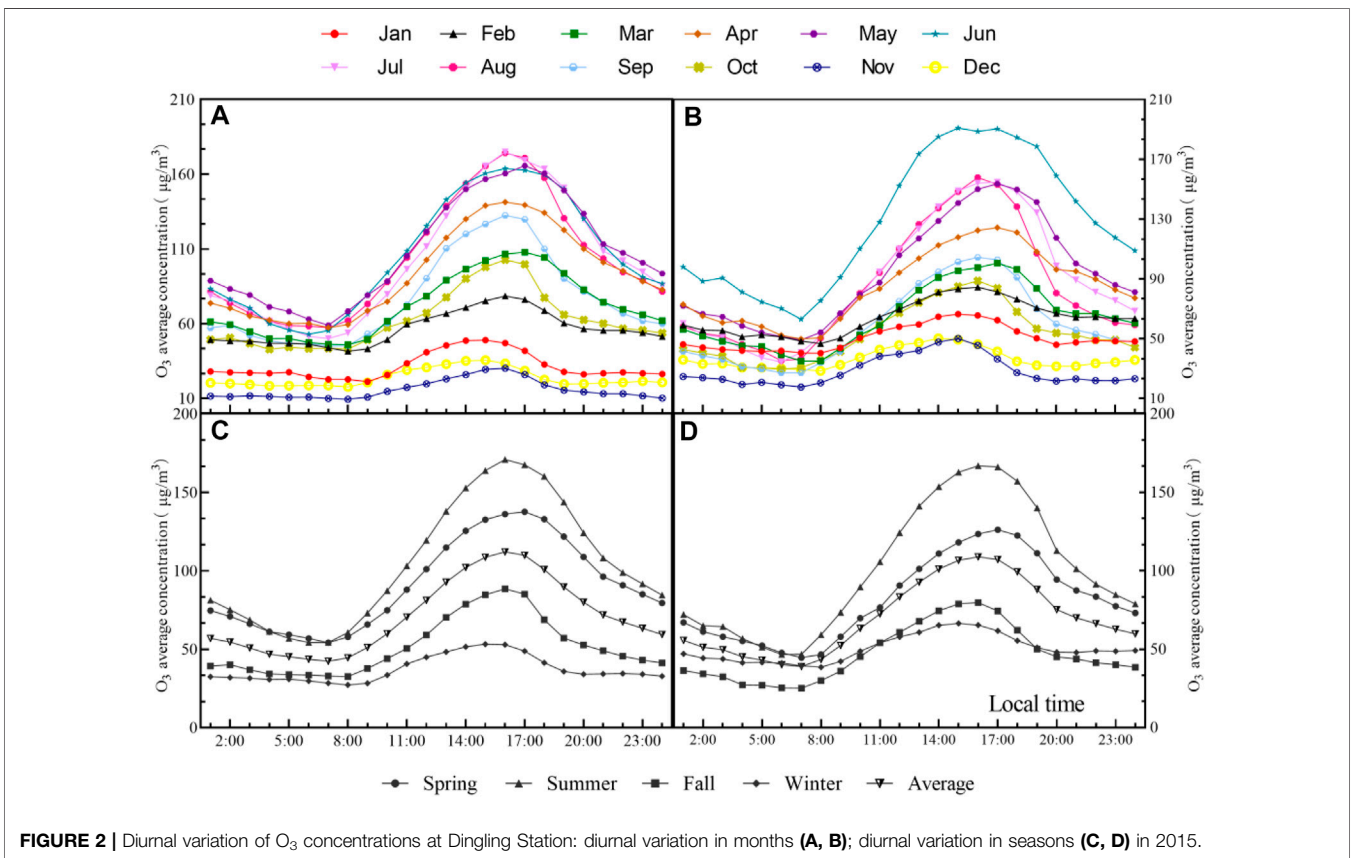
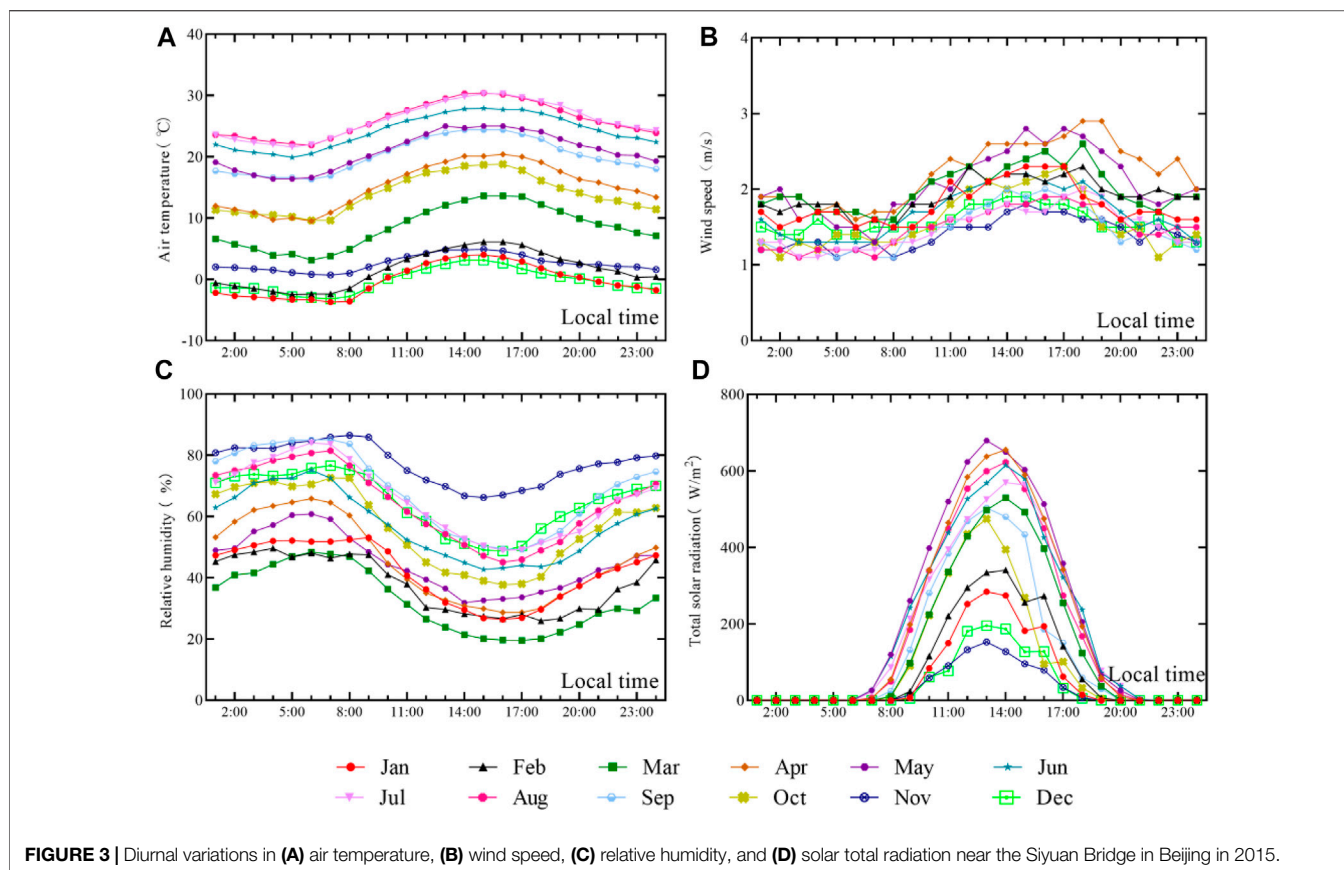
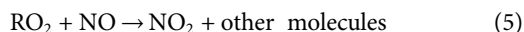


FIGURE 2 | Diurnal variation of O<sub>3</sub> concentrations at Dingling Station: diurnal variation in months (A, B); diurnal variation in seasons (C, D) in 2015.



oxides are the key precursors (Zaveri et al., 2003; Wang et al., 2019). The chemical processes of ozone generated by nitrogen oxides and VOCs can be described by following equations (Sillman and He, 2002; Khalil, 2018).



Previous studies have shown that  $\text{O}_3$  in the atmosphere is mainly produced by the photochemical processes of precursors such as nitrogen oxides ( $\text{NO}_x$ ), carbon monoxide ( $\text{CO}$ ), and VOCs that are emitted by humans and nature, and the  $\text{O}_3$  formation process is also accompanied by the production of many oxidants such as peroxyacetyl nitrate (PAN) (Berntsen et al., 1996; An, 2017). In addition to a direct relationship with the precursor emissions, the  $\text{O}_3$  concentration in the atmosphere is closely related to meteorological conditions such as atmospheric temperature, solar radiation, wind direction and speed, and atmospheric stratification stability (Lin et al., 2008). Air temperature and solar radiation affect the photochemical reaction intensity and the wind direction and speed; atmospheric stratification stability affects transmission and diffusion (Huang et al., 2019). It should be noted that the source of the precursors is very complicated. For example,  $\text{NO}_x$  mainly comes

from motor vehicle exhaust and the combustion process of coal and power plant oil; the VOCs come from sources such as petrochemical production, painting, and cooking and natural emissions from vegetation (Hata and Tonokura, 2019). Therefore, it is very difficult to control  $\text{O}_3$ . Although the  $\text{O}_3$  concentration is largely determined by locally emitted  $\text{O}_3$  precursors, the  $\text{O}_3$  has a few weeks of life in the troposphere once it is generated, and will be transmitted over long distances. Therefore, atmospheric  $\text{O}_3$  pollution has become a worldwide challenge.

With the rapid development of the economy and urbanization, human activities emit a large amount of  $\text{NO}_x$ ,  $\text{CO}$ , and nonmethane hydrocarbons into the atmosphere, consequently these pollutants produce high  $\text{O}_3$  concentrations under suitable meteorological conditions (Wang et al., 2014).

Investigations present that  $\text{O}_3$  concentration shows an increasing trend during the past decades and will continuously increase in future in eastern China (Ma et al., 2016; Sun et al., 2016; Wang et al., 2020). The *China Environmental Status Bulletin* has announced that the high concentrations of near-surface atmospheric  $\text{O}_3$  are the primary air pollutant in China's "Beijing-Tianjin-Hebei", "Yangtze River Delta", and "Pearl River Delta" regions during the summer since 2015. Beijing is the megacity, with over ten million people, and has exhibited rapid economic development. By the end of 2018, the city's permanent population has exceeded 20 million, and the number of motor vehicles has kept steadily increasing with approximately 6 million. The dense population and high number of motor vehicles have contributed to very poor air quality in Beijing. As a result, the near-surface

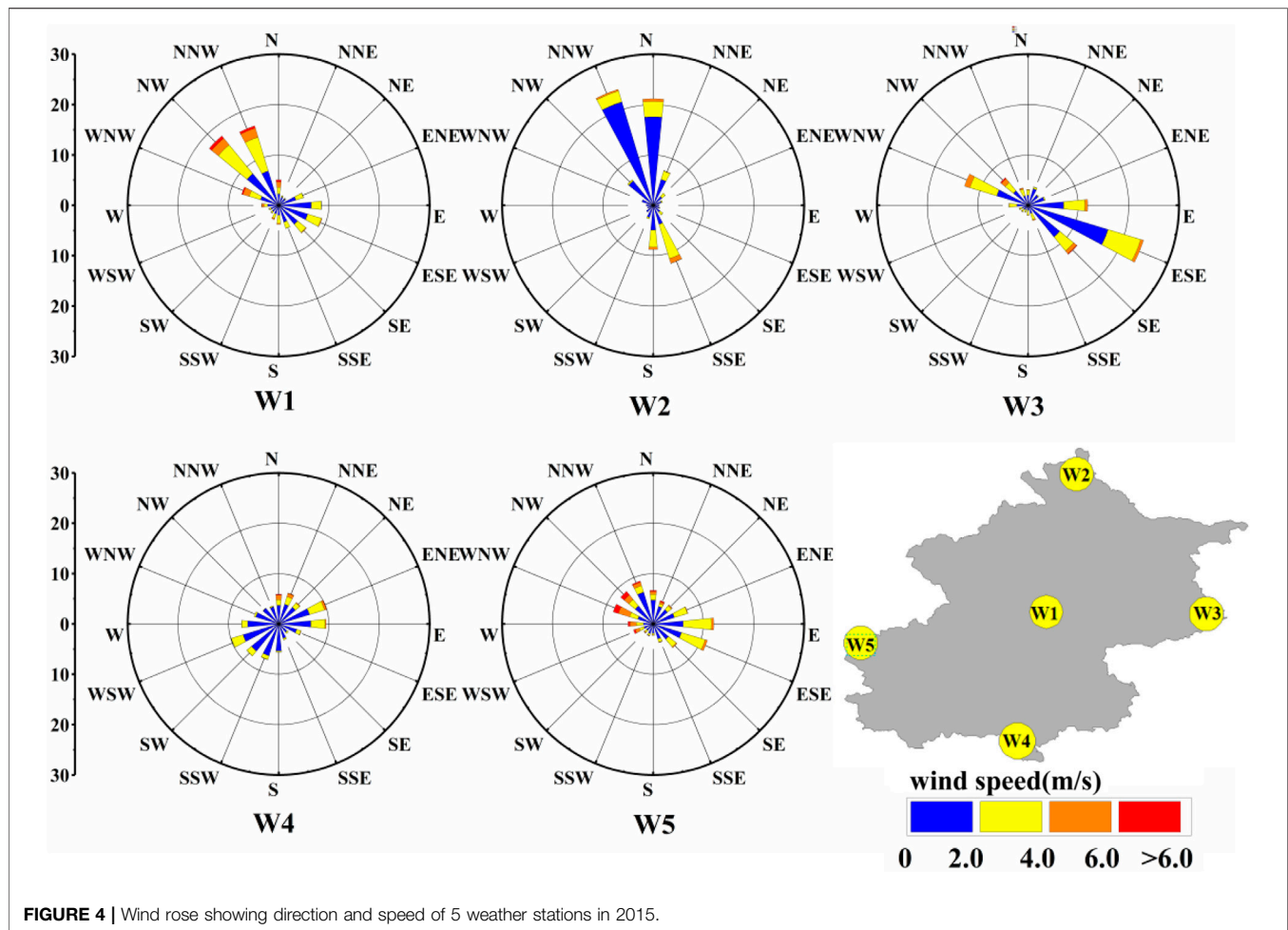


FIGURE 4 | Wind rose showing direction and speed of 5 weather stations in 2015.

atmospheric  $O_3$  concentrations and the number of days exceeding the standard have shown a significant upward trend in the past three years (Cheng et al., 2017; Zhang and Zhang, 2019). Therefore, factors of influencing  $O_3$  formation and spatiotemporal distribution of  $O_3$  concentration need to be better understood to take measures for  $O_3$  control (Cheng et al., 2018; Yang et al., 2020; Zhao et al., 2020).

However, the spatiotemporal dynamics and influencing factors of near-surface  $O_3$  concentration in Beijing are not clear. In this study, we use hourly  $O_3$  data at 33 air quality automatic monitoring stations in Beijing in 2015 and 2018 to systematically explore the spatiotemporal characteristics of near-surface  $O_3$  concentrations, and the role of the environment factors including vegetation in influencing  $O_3$  concentration. The results will provide data support and direction for relevant environmental governance.

## DATA AND ANALYSIS METHOD

### Data Sources

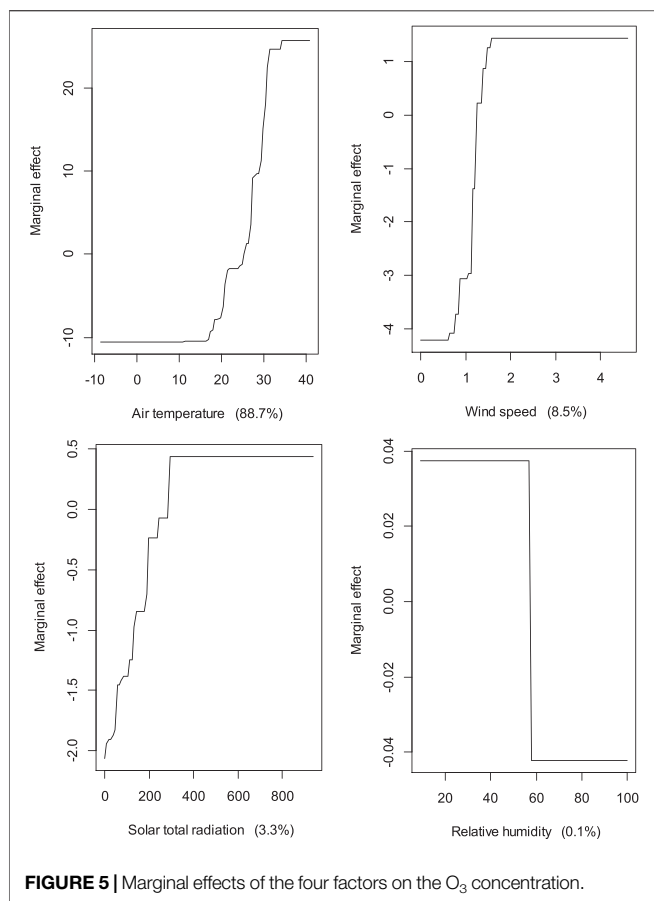
The near-surface hourly  $O_3$  concentration data in 2015 and 2018 were from the Beijing Environmental Protection Monitoring Center (<http://www.bjmemc.com.cn/>). They were observed by

thermo fisher 49C ultraviolet photometers, which were installed at 33 ground air quality monitoring stations (Wang et al., 2014). According to the environmental protection standards of the People's Republic of China (HJ664–2013): *Technical Regulation for Selection of Ambient Air Quality Monitoring Stations* (Trial), each air quality monitoring station has a typical area radius of 500–4 km. There are no tall buildings, trees, or other obstacles around the monitoring equipment sampling port that could impede air circulation. Also, there should be no obvious fixed sources of pollution within at least 50 m (**Supplementary Table S1** in Supplementary Material).

According to the different monitoring functions, the 33 stations can be divided into urban environmental assessment points (A1–A11), suburban environmental assessment points (B1–B11), background control point (C1), regional transmission monitor points (D1–D6), and traffic pollution monitor points (E1–E4).

The 33 stations are located in the urban districts (Dongcheng, Xicheng, Chaoyang, Haidian, Fengtai, and Shijingshan), northwestern districts (Changping and Yanqing), northeastern districts (Huairou, Miyun, Pinggu, and Shunyi), southeastern district (Tongzhou, Daxing, and Yizhuang), and southwestern districts (Fangshan and Mentougou), which cover all the urban and suburb districts in Beijing (**Figure 1**).





Meteorological data from the DYNAMET scientific-grade automatic weather station near the Siyuan Bridge in Beijing was selected to analyze 2015 diurnal variations in air temperature, wind speed, relative humidity, and solar total radiation. Other meteorological data used came from the automatic weather station of the Beijing Meteorological Bureau. The weather observations were carried out according to national standards of the People's Republic of China (GB/T 35,221–2017): *Specifications for surface meteorological observation-general*, and the precision of air temperature, relative humidity, wind speed is 0.1°C, 1%, 0.1 m/s, respectively.

## Data Preprocessing

Prior to use of the data, an adjacent interpolation filling was performed for the individual missing data caused by equipment failure, when there are less than or equal to three consecutive missing measurement data, they are filled by arithmetical sequence, while other cases are filled by the averaged value of three adjacent stations at the same time.

## RESULTS AND DISCUSSION

### Diurnal Variation Characteristics of Near-Surface O<sub>3</sub> Concentration

The diurnal near-surface O<sub>3</sub> concentration variations at 33 stations have a similar pattern, therefore, for brevity we just

take C1 station as an example to describe it. **Figure 2A,B** show that the diurnal curve for each month has a similar pattern in 2015, that is, near-surface O<sub>3</sub> concentration was lowest at 06:00 to 07:00, then rose rapidly to the maximum value at 14:00 to 15:00, after that it declined until the next morning. **Figure 2C,D** show that the diurnal variation for each season is consistent with the other researches Wang et al. (2014), Cheng et al. (2016), and its main influencing factors may be related to air temperature and solar radiation.

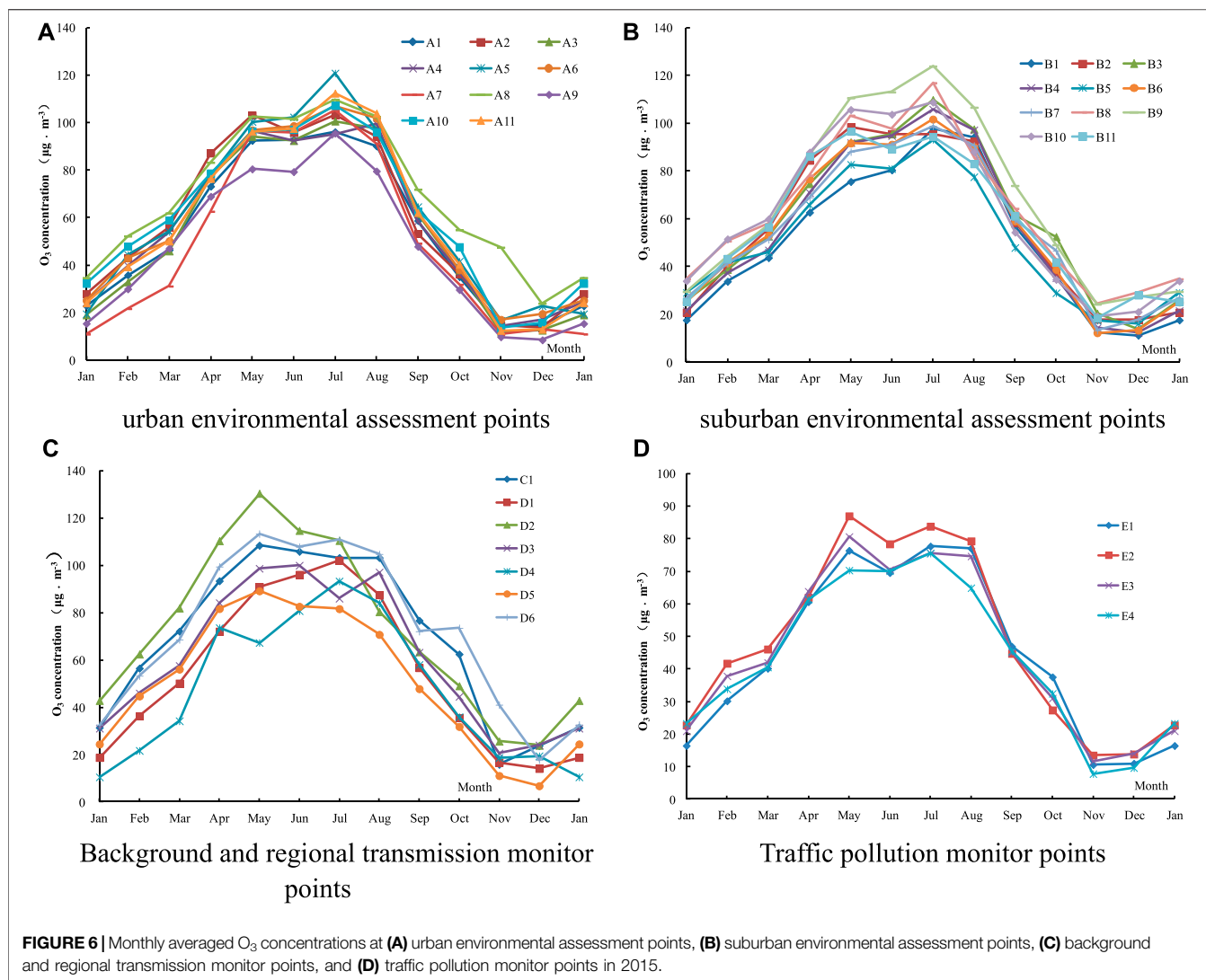
By comparing **Figure 2**; **Figure 3**, we found that the diurnal variations of near-surface O<sub>3</sub> concentration are similar to those of surface air temperature, wind speed, and solar total radiation. We selected July in C1 station as an example to analyze their relationships. According to Spearman correlation analysis, the correlation coefficients of the O<sub>3</sub> concentration with temperature, solar total radiation, and wind speed were 0.925, 0.629, and 0.932, respectively, with a significant positive correlation ( $P < 0.01$ ). On the other hand, the O<sub>3</sub> concentration has a negative correlation with relative humidity with the correlation coefficient of  $-0.977$ . The results are substantially consistent with the conclusions of the other studies (Xu and Zhu, 1994; An, 2017). The negative correlation may come from the following reasons. Firstly, when the relative humidity increases, it is often accompanied by an increase in cloudiness, which is detrimental to O<sub>3</sub> generation and results in a decrease in the O<sub>3</sub> concentration (Zhao et al., 2019). Secondly, related studies on chemical mechanisms suggest that in heavily polluted urban areas, the increase in water vapor drives the conversion of NO<sub>2</sub> to nitric acid because of the large amount of O<sub>3</sub> precursors, thereby inhibiting the formation of O<sub>3</sub> (Camalier et al., 2007; Jacob and Winner, 2009).

Based wind direction frequency rose map (**Figure 4**) for five meteorological stations (located in the northern, southern, eastern, southwestern and central regions of Beijing, respectively), there are differences in the dominant wind directions of the five meteorological stations in 2015, about northern in Beijing, the dominating wind direction is NW, and southern is SW, atmospheric O<sub>3</sub> from other cities transport is not easy to diffuse.

Furthermore, boosted regression trees (BRT) model was used to analyze the relative contribution and marginal effects of independent variables on dependent variables. In this study, the atmospheric O<sub>3</sub> concentration in 2015 at the Olympic Center station were randomly selected as the dependent variable, and the air temperature, wind speed, solar total radiation and relative humidity obtained from neighboring weather stations were used as independent variables.

The BRT model was developed using the R software with the packages “gbm” (Ridgeway, 2015) and “brt.functions.R” (Elith et al., 2008). The BRT model was fitted with the following parameters: a learning rate of 0.005, a bag fraction of 0.5, a tree complexity of 5, and fivefold cross-validation.

The result indicated that the correlation of the training data was 0.82. Among the four meteorological factors affecting the O<sub>3</sub> concentration, air temperature play a dominant role in influencing the O<sub>3</sub> concentration (the relative contribution is more than 88%). On the other hand, the relative contributions of



wind speed, solar total radiation and relative humidity are 8.5, 3.3, and 0.1%, respectively.

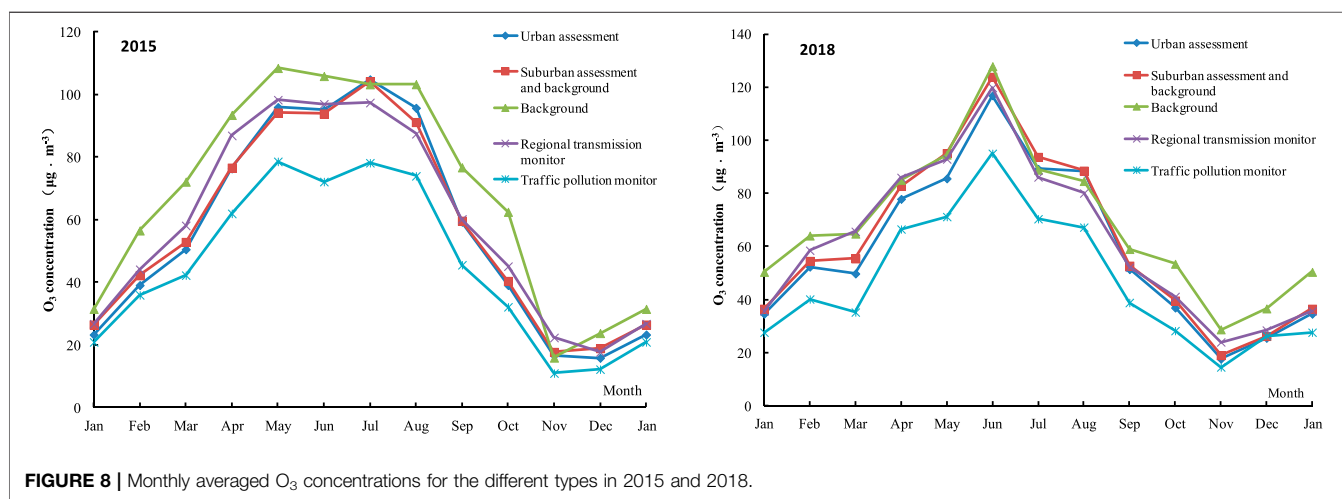
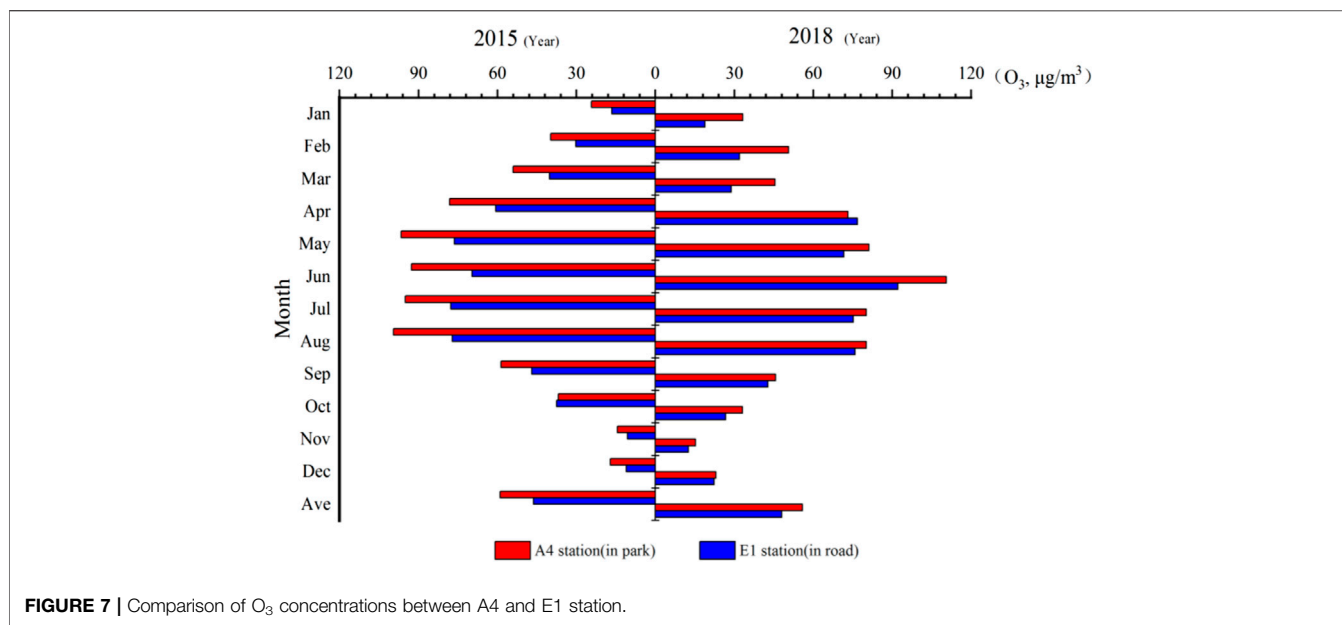
The marginal effects of the four factors (air temperature, wind speed, solar total radiation and relative humidity) on the O<sub>3</sub> concentration were further analyzed, the marginal effect was calculated by holding all the other variables at their averaged values, as the air temperature increases, the O<sub>3</sub> concentration shows a significant increasing trend (Figure 5).

### Annual Variation Characteristics of Near-Surface O<sub>3</sub> Concentration

As shown in Figure 6, the monthly averaged characteristics of O<sub>3</sub> concentration at the 33 monitoring stations were mostly similar, showing a distinct “bell-shaped” unimodal distribution. The highest value generally appeared in the summer from June to August, and the lowest value generally occurred in January during the winter. The highest monthly averaged O<sub>3</sub> concentration observed in Beijing in 2015 exceeded 130.0 µg·m<sup>-3</sup>; while the

lowest value was less than 20.0 µg·m<sup>-3</sup>. The annual variations of O<sub>3</sub> concentration in 2018 had very similar characteristics to those in 2015 but with larger values.

There are three main reasons for the seasonal variation in atmospheric O<sub>3</sub> concentration: first, the large temperature difference between the winter and summer in Beijing leads to seasonal differences in O<sub>3</sub> concentration because of the good positive correlation between the O<sub>3</sub> concentration and the near-surface atmosphere temperature. On the other hand, winter, the haze-prone period, has a higher concentration of particulate matter, which leads to an increase in the aerosol optical thickness, weak photochemical reactions, and a decrease in the O<sub>3</sub> concentration, and the heterogeneous chemical reaction of particulate matter in winter also causes O<sub>3</sub> consumption (Deng et al., 2011). In addition, it may be related to vegetation. By comparing A4 station (located in urban park, which has vegetation cover area of 4.5 ha) and E1 station (located in road, which is adjacent to A4 station), due to the relatively large volatile organic compounds emissions of plants, which



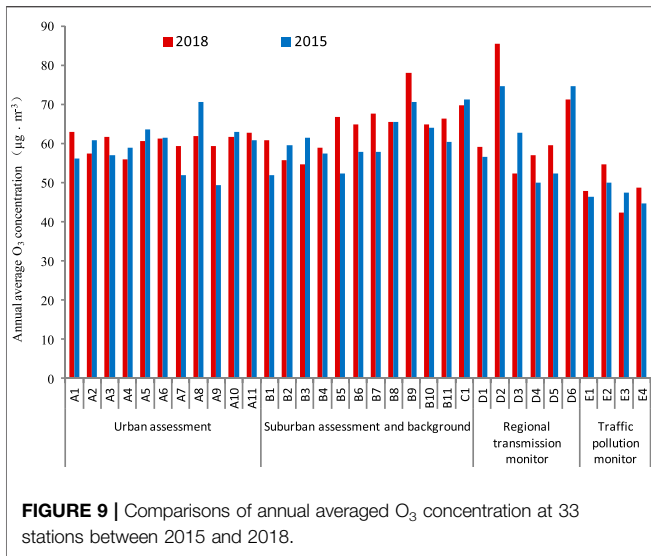
indirectly promotes the O<sub>3</sub> formation, the annual averaged O<sub>3</sub> concentration at A4 station in 2015 and 2018 was 28 and 16% higher than E1 station, respectively, (Figure 7).

As shown in Figure 8, the averaged O<sub>3</sub> concentrations at the traffic pollution control points for all months were significantly lower than that of the other four types. we determined the 2015 averaged O<sub>3</sub> concentration, in order from highest to lowest, of the background control point (71.2 µg m<sup>-3</sup>), regional transmission monitor point (61.9 µg m<sup>-3</sup>), suburban environmental assessment point (60.0 µg m<sup>-3</sup>), urban environmental assessment point (59.4 µg m<sup>-3</sup>), and traffic pollution monitor point (47.1 µg m<sup>-3</sup>); the same size sequence was also presented in 2018, and other studies have similar phenomena (Zhang et al., 2014). This is primarily related to the high NO concentration of vehicle exhaust emissions near the traffic pollution control points. Relevant research indicates that there is a photostable relationship among O<sub>3</sub>, NO, and NO<sub>2</sub> (An, 2017);

the NO concentration is high, which is not conducive to O<sub>3</sub> formation in the atmosphere, and continues to “titrate” and consume atmospheric O<sub>3</sub> through the reaction (Lin et al., 2007; Cheng et al., 2016).

### Annual Averaged O<sub>3</sub> Concentration

The annual averaged O<sub>3</sub> concentration (value ± standard deviation) in Beijing was 58.9 ± 7.9 µg·m<sup>-3</sup> in 2015 (Supplementary Table S2 in Supplemental Materials). Tang et al. (2009) studied the O<sub>3</sub> concentration characteristics in Beijing from 2001 to 2006, and found that the averaged O<sub>3</sub> concentration during the six years in Beijing was 53.2 ± 11.8 µg·m<sup>-3</sup>. Among the 33 monitoring stations, the lowest annual averaged O<sub>3</sub> concentration appeared at the E4 Station (44.7 µg·m<sup>-3</sup>, which is a traffic pollution monitor point) in the central city of Beijing. The highest annual averaged O<sub>3</sub> concentration



appeared at the D2 station (74.7 μg·m<sup>-3</sup>, which is a regional transmission monitor point) located in northeastern Beijing.

**Figure 9** shows that the annual averaged O<sub>3</sub> concentrations at most of the monitoring stations in 2018 were larger than those in 2015. Consequently, the averaged value for 33 stations was 61.2 ± 8.2 μg·m<sup>-3</sup> in 2018, which was higher than that in 2015. The lowest averaged O<sub>3</sub> concentration in 2018 appeared at the E3 station (42.4 μg·m<sup>-3</sup>), which is also a traffic pollution monitor point, while the highest value still appeared at the D2 (85.5 μg·m<sup>-3</sup>).

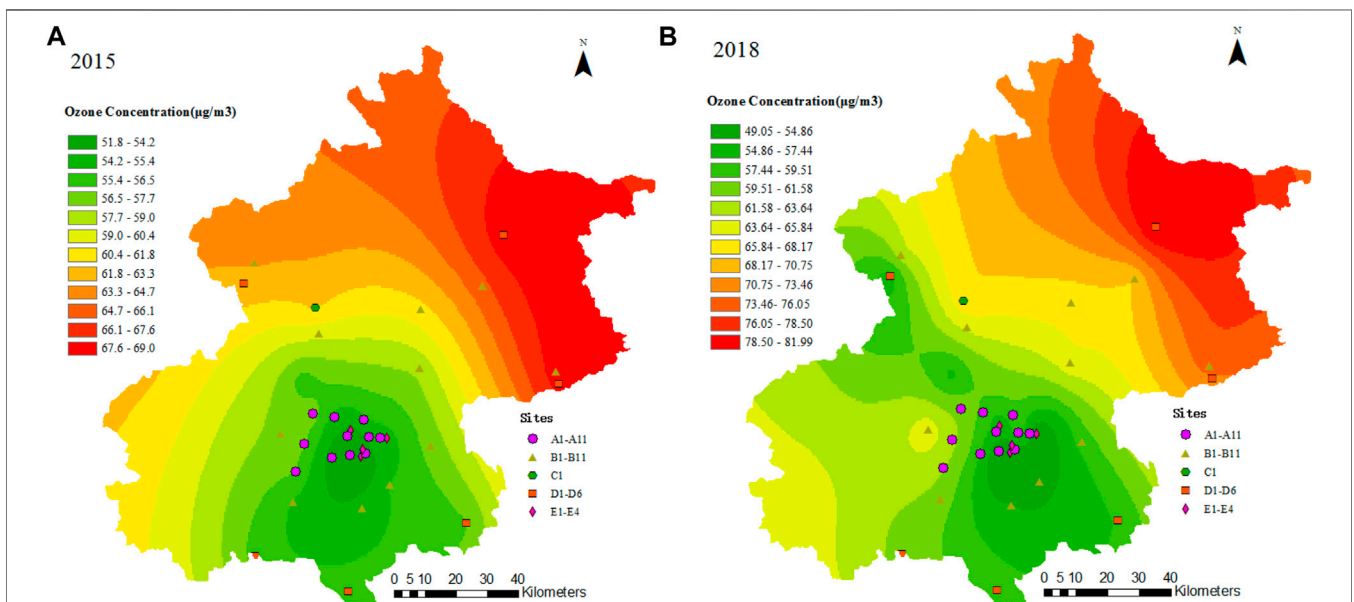
The reason that the lower annual averaged O<sub>3</sub> concentration appeared at traffic pollution monitor point both in 2015 and 2018 is likely related to the high NO concentration from the vehicles emission near the traffic station.

The occurrence of the highest value at D2 station may be caused by following reasons: first, the vegetation coverage rate of the D2 is high, and the VOCs emitted by the plants are favorable for the generation of O<sub>3</sub>. Second, the atmospheric regional transmission and the unique terrain of Beijing affect the values, and the local wind is prevalent in Beijing when strong weather systems pass through the territory. The O<sub>3</sub> precursors discharged in the urban area of Beijing are usually transmitted to the northern mountainous areas during the daytime, and photochemical reactions gradually occur during the transportation, resulting in a higher level of O<sub>3</sub> in the downwind direction than that in urban areas (Wang et al., 2006; Ma et al., 2011; Cheng et al., 2016). Third, atmospheric particulate matter concentration can also play an important role in influencing O<sub>3</sub> concentration. For example, Li et al. (2019) found that the PM2.5 concentration in the summer of the past five years has decreased by approximately 40%, which is an important factor leading to the increase in O<sub>3</sub> concentration during the summer in the North China Plain, this factor increases the solar radiation intensity and reduces the heterogeneous absorption of HO<sub>2</sub> radicals by aerosols, which in turn increases the formation of O<sub>3</sub>. With a lower concentration of atmospheric particulate matter in the area where D2 station is located Cheng et al. (2015), it is beneficial to the generation of O<sub>3</sub>.

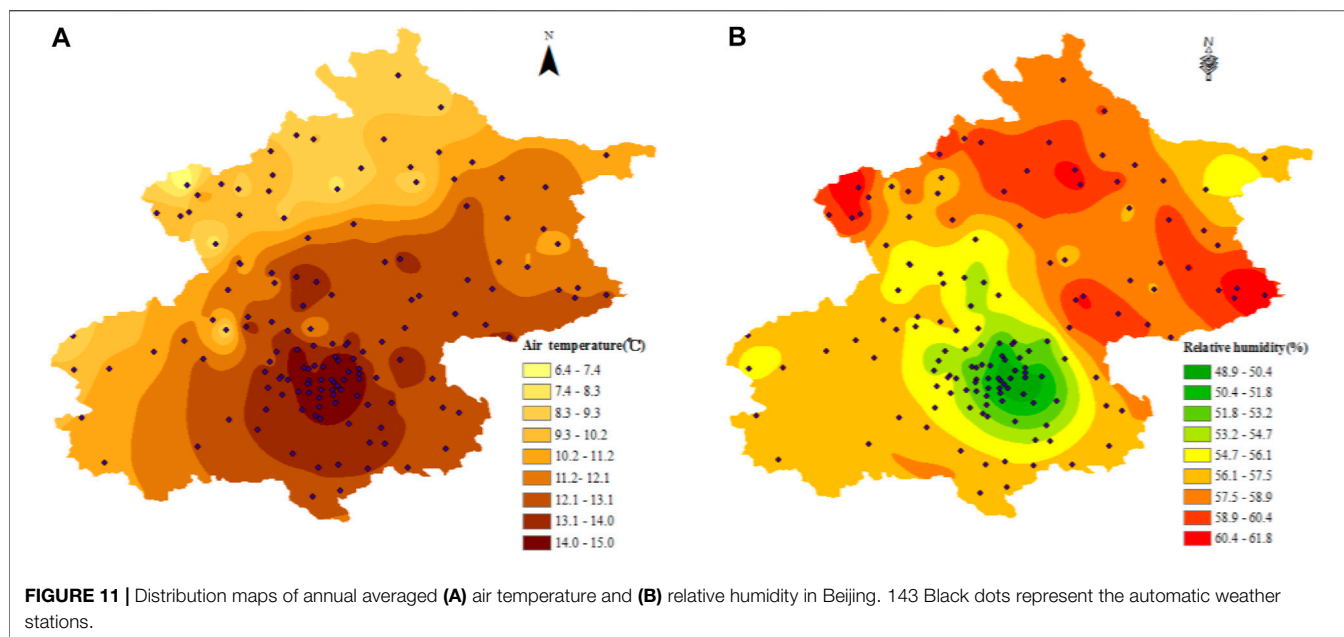
It is worth to note that although the annual averaged O<sub>3</sub> concentration for most stations in Beijing increased in 2018 relative to 2015, the reduced O<sub>3</sub> concentration in the near-surface atmosphere still occurred at a small number of monitoring stations. The phenomenon and possible reasons are worthy of further research.

### Spatial Distribution Characteristics of Near-Surface O<sub>3</sub> Concentration

To perform spatial interpolation, we clicked ArcToolbox and selected “Kriging” under “Spatial analyst tools” in the “Arcmap







10" software. From the spatial interpolation map (Figure 10), the annual averaged O<sub>3</sub> concentrations were relatively low in the central areas and southern districts/counties of Beijing. By contrast, the O<sub>3</sub> concentrations were relatively high in the northern districts/counties, especially in the northeastern part where there is excellent ecological vegetation and the annual averaged O<sub>3</sub> concentration is the highest. This is basically consistent with the spatial distribution characteristics obtained by Wang et al. (2014).

Although the northeastern area has a higher altitude (1,000–1,500 m), lower annual averaged temperature, and higher relative humidity (Figure 11), which are not conducive to the photochemical reaction of atmospheric O<sub>3</sub>, the vegetation coverage in this area is high (Figure 1), where the amount of VOCs emitted by plants is higher, and the lower concentration of atmospheric particulate matter maybe is conducive to the generation of O<sub>3</sub>. In addition, the higher annual averaged O<sub>3</sub> concentration over the area could be affected by the atmospheric regional transmission.

## CONCLUSION

The diurnal variation in near-surface O<sub>3</sub> concentrations for each month, season, and year showed a unimodal variation at 33 monitoring stations in 2015 and 2018. The O<sub>3</sub> concentration usually reached the lowest value from 06:00 to 07:00, and then rose rapidly to the maximum at 14:00 to 15:00, and then declined until the early morning of the next day. Although the daily variation curve of the O<sub>3</sub> concentration does not conform to the normal distribution, it is similar to the daily variation curves of temperature, wind speed, and solar total radiation.

Spearman correlation analysis showed that the correlation coefficients of O<sub>3</sub> concentration with temperature, solar total radiation, and wind speed were 0.925, 0.629, and 0.932, respectively, with a significant positive correlation ( $P < 0.01$ ), while the correlation coefficient with air relative humidity was  $-0.977$ , which showed a significant negative correlation. Furthermore, the relative contributions of environmental factors to the O<sub>3</sub> concentration were analyzed by the boosted regression trees model, it is revealed that the air temperature was the main influencing factor (relative contributions > 88%). On the other hand, the relative contributions of wind speed, solar total radiation and relative humidity are 8.5, 3.3, and 0.1%, respectively.

The monthly averaged change characteristic of the O<sub>3</sub> concentration show a distinct "bell-shaped" unimodal distribution at the 33 monitoring stations in 2015 and 2018. The highest value generally appeared from June to August during the summer, and the lowest value generally occurred in January during the winter. The highest monthly averaged O<sub>3</sub> concentration that was observed in 2015 exceeded  $130.0 \mu\text{g}\cdot\text{m}^{-3}$ , and the lowest value was less than  $20.0 \mu\text{g}\cdot\text{m}^{-3}$ .

The annual averaged O<sub>3</sub> concentration (value  $\pm$  standard deviation) in Beijing was  $58.9 \pm 7.9 \mu\text{g}\cdot\text{m}^{-3}$  in 2015, and increased to  $61.2 \pm 8.2 \mu\text{g}\cdot\text{m}^{-3}$  in 2018. Among the 33 monitoring stations, the lowest annual averaged O<sub>3</sub> concentration in 2018 appeared at the E3 station ( $42.4 \mu\text{g}\cdot\text{m}^{-3}$ ), which belongs to the traffic pollution control point. This is likely related to the high NO concentration of vehicle exhaust emissions near the traffic station. The highest value appeared at the D2 station ( $85.5 \mu\text{g}\cdot\text{m}^{-3}$ ) in northeastern Beijing, which belongs to the regional background transmission point. The occurrence of the highest value should be primarily related to vegetation coverage, atmospheric regional transmission, and atmospheric particulate matter concentration.

As shown in the spatial interpolation map, the annual averaged O<sub>3</sub> concentrations were relatively low in the central areas and southern districts/counties of Beijing, while the values were relatively high in the northern districts/counties in both 2015 and 2018, especially in the northeastern part that contained excellent ecological vegetation with the highest annual averaged O<sub>3</sub> concentration. Although the northeastern area has a lower annual averaged temperature and higher relative humidity, which are not conducive to the photochemical reaction of atmospheric O<sub>3</sub>, the vegetation coverage in this area is high. Moreover, the amount of VOCs emitted by plants is higher, and the lower concentration of atmospheric particulate matter is conducive to the generation of O<sub>3</sub>. The higher averaged O<sub>3</sub> concentration in the area may be also affected by the atmospheric regional transmission.

## DATA AVAILABILITY STATEMENT

The original contributions presented in the study are included in the article/**Supplementary Material**, further inquiries can be directed to the corresponding author.

## REFERENCES

- An, J. L. (2017). Study on the Variation Characteristics of Surface Ozone Concentrations and its Production in Beijing. Doctoral dissertation. Nanjing, China: Nanjing University of Information Science and Technology. [In Chinese]. doi:10.7666/d.y1257767
- Berntsen, T., Isaksen, I. S. A., Wang, W.-C., and Liang, X.-Z. (1996). Impacts of Increased Anthropogenic Emissions in Asia on Tropospheric Ozone and Climate. *Tellus B: Chem. Phys. Meteorology* 48 (1), 13–32. doi:10.3402/tellusb.v48i1.15662
- Calafapietra, C., Scarascia Mugnozza, G., Karnosky, D. F., Loreto, F., and Sharkey, T. D. (2008). Isoprene Emission Rates under Elevated CO<sub>2</sub> and O<sub>3</sub> in Two Field-grown Aspen Clones Differing in Their Sensitivity to O<sub>3</sub>. *New Phytol.* 179 (1), 55–61. doi:10.1111/j.1469-8137.2008.02493.x
- Camalier, L., Cox, W., and Dolwick, P. (2007). The Effects of Meteorology on Ozone in Urban Areas and Their Use in Assessing Ozone Trends. *Atmos. Environ.* 41 (33), 7127–7137. doi:10.1016/j.atmosenv.2007.04.061
- Cheng, L. J., Wang, S., Gong, Z. Y., Yang, Q., and Wang, Y. Q. (2017). Pollution Trends of Ozone and its Characteristics of Temporal and Spatial Distribution in Beijing-Tianjin-Hebei Region. *J. Environ. Monit. China* 33 (1), 14–21. [In Chinese]. doi:10.19316/j.jissn.1002-6002.2017.01.03
- Cheng, L., Wang, S., Gong, Z., Li, H., Yang, Q., and Wang, Y. (2018). Regionalization Based on Spatial and Seasonal Variation in Ground-Level Ozone Concentrations across China. *J. Environ. Sci.* 67, 179–190. doi:10.1016/j.jes.2017.08.011
- Cheng, N. L., Li, Y. T., Zhang, D. W., Sun, R. W., Dong, X., Cheng, B. F., et al. (2015). Analysis on the Spatial and Temporal Distribution of pm<sub>2.5</sub> in Beijing in 2013. *J. Environ. Eng.* 33 (10), 43–46. [In Chinese]. doi:10.13205/j.hjgc.201510010
- Cheng, N. L., Li, Y. T., Zhang, D. W., Chen, T., Wei, Q., Sun, T. H., et al. (2016). Characteristics of Ozone Background Concentration in Beijing from 2004 to 2015. *Huan Jing Ke Xue* 37 (8), 2847–2854. [In Chinese]. doi:10.13227/j.hjkk.2016.08.004
- Deng, X., Zhou, X., Wu, D., Tie, X., Tan, H., Li, F., et al. (2011). Effect of Atmospheric Aerosol on Surface Ozone Variation over the Pearl River Delta Region. *Sci. China Earth Sci.* 54 (5), 744–752. doi:10.1007/s11430-011-4172-7
- Elith, J., Leathwick, J. R., and Hastie, T. (2008). A Working Guide to Boosted Regression Trees. *J. Anim. Ecol.* 77 (4), 802–813. doi:10.1111/j.1365-2656.2008.01390.x

## AUTHOR CONTRIBUTIONS

JX collected all the data, performed all data analysis, and developed the entire draft manuscript. SS and XZ participated in the experimental design, developed many tables and figures, and provided many edits on the manuscript, including references and citations. LW designed the study plan, performed data preprocessing and provided many edits on the manuscript, including references and citations.

## FUNDING

This research was supported by the project for National Natural Science Foundation of China (31770751 and 41675085).

## SUPPLEMENTARY MATERIAL

The Supplementary Material for this article can be found online at: <https://www.frontiersin.org/articles/10.3389/fenvs.2021.593220/full#supplementary-material>

- Hata, H., and Tonokura, K. (2019). Impact of Next-Generation Vehicles on Tropospheric Ozone Estimated by Chemical Transport Model in the Kanto Region of Japan. *Sci. Rep.* 9 (1), 3573. doi:10.1038/s41598-019-40012-y
- Huang, X. G., Zhao, J. B., Cao, J. J., and Song, Y. Y. (2019). Spatial-temporal Variation of Ozone Concentration and its Driving Factors in China. *Huan Jing Ke Xue* 40 (3), 1120–1131. [In Chinese]. doi:10.13227/j.hjkk.201807038
- Jacob, D. J., and Winner, D. A. (2009). Effect of Climate Change on Air Quality. *Atmos. Environ.* 43 (1), 51–63. doi:10.1016/j.atmosenv.2008.09.051
- Khalil, M. A. K. (2018). Steady States and Transport Processes in Urban Ozone Balances. *Npj Clim. Atmos. Sci.* 1, 22. doi:10.1038/s41612-018-0035-7
- Kong, Q. X., Liu, G. R., and Li, G. C. (1999). Surface Ozone Concentration Variation and Possible Influences on Human Health. *J. Climatic Environ. Res.* 4 (1), 61–66. [In Chinese]. doi:10.3878/j.jissn.1006-9585.1999.01.14
- Lehman, J., Swinton, K., Bortnick, S., Hamilton, C., Baldrige, E., Eder, B., et al. (2004). Spatio-temporal Characterization of Tropospheric Ozone across the Eastern United States. *Atmos. Environ.* 38 (26), 4357–4369. doi:10.1016/j.atmosenv.2004.03.069
- Li, K., Jacob, D. J., Liao, H., Shen, L., Zhang, Q., and Bates, K. H. (2019). Anthropogenic Drivers of 2013–2017 Trends in Summer Surface Ozone in China. *Proc. Natl. Acad. Sci. USA* 116 (2), 422–427. doi:10.1073/pnas.1812168116
- Lin, C.-Y., Wang, Z., Chou, C. C.-K., Chang, C.-C., and Liu, S. C. (2007). A Numerical Study of an Autumn High Ozone Episode over Southwestern Taiwan. *Atmos. Environ.* 41 (17), 3684–3701. doi:10.1016/j.atmosenv.2006.12.050
- Lin, W., Xu, X., Zhang, X., and Tang, J. (2008). Contributions of Pollutants from North China Plain to Surface Ozone at the Shangdianzi GAW Station. *Atmos. Chem. Phys.* 8, 5889–5898. doi:10.5194/acp-8-5889-2008
- Loreto, F., and Schnitzler, J.-P. (2010). Abiotic Stresses and Induced BVOCs. *Trends Plant Sci.* 15 (3), 154–166. doi:10.1016/j.tplants.2009.12.006
- Ma, Z. Q., Wang, Y. S., Zhang, X. L., and Xu, J. (2011). Comparison of Ozone between Beijing and Downstream Area. *Huan Jing Ke Xue* 32 (4), 924–929. [In Chinese].
- Ma, Z., Xu, J., Quan, W., Zhang, Z., Lin, W., and Xu, X. (2016). Significant Increase of Surface Ozone at a Rural Site, North of Eastern China. *Atmos. Chem. Phys.* 16, 3969–3977. doi:10.5194/acp-16-3969-2016
- Raddatz, R. L., and Cummine, J. D. (2001). Temporal Surface Ozone Patterns in Urban Manitoba, Canada. *Boundary-Layer Meteorology* 99 (3), 411–428. doi:10.1023/A:101898301216810.1023/a:1018983012168

- Ridgeway, G. (2015). Generalized Boosted Regression Models. R package version 2.1.1 [DB/OL]. Available at: <https://github.com/harrysouthworth/gbm> (Accessed April 29, 2021).
- Sillman, S., and He, D. Y. (2002). Some Theoretical Results Concerning O<sub>3</sub>-NO<sub>x</sub>-VOC Chemistry and NO<sub>x</sub>-VOC Indicators. *J. Geophys. Res.* 107 (D22), 4659. doi:10.1029/2001JD001123
- Sun, L., Xue, L., Wang, T., Gao, J., Ding, A., Cooper, O. R., et al. (2016). Significant Increase of Summertime Ozone at Mount Tai in Central Eastern China. *Atmos. Chem. Phys.* 16, 10637–10650. doi:10.5194/acp-16-10637-2016
- Tang, G., Li, X., Wang, Y., Xin, J., and Ren, X. (2009). Surface Ozone Trend Details and Interpretations in Beijing, 2001–2006. *Atmos. Chem. Phys.* 9, 8813–8823. doi:10.5194/acp-9-8813-2009
- Velikova, V., Pinelli, P., Pasqualini, S., Reale, L., Ferranti, F., and Loreto, F. (2005). Isoprene Decreases the Concentration of Nitric Oxide in Leaves Exposed to Elevated Ozone. *New Phytol.* 166 (2), 419–426. doi:10.1111/j.1469-8137.2005.01409.x
- Wang, T., Ding, A., Gao, J., and Wu, W. S. (2006). Strong Ozone Production in Urban Plumes from Beijing, China. *Geophys. Res. Lett.* 33, 21806. doi:10.1029/2006GL027689
- Wang, T., Xue, L., Brimblecombe, P., Lam, Y. F., Li, L., and Zhang, L. (2017). Ozone Pollution in China: A Review of Concentrations, Meteorological Influences, Chemical Precursors, and Effects. *Sci. Total Environ.* 575, 1582–1596. doi:10.1016/j.scitotenv.2016.10.081
- Wang, Y., Gao, W., Wang, S., Song, T., Gong, Z., Ji, D., et al. (2020). Contrasting Trends of PM<sub>2.5</sub> and Surface-Ozone Concentrations in China from 2013 to 2017. *Natl. Sci. Rev.* 7, 1331–1339. doi:10.1093/nsr/nwaa032
- Wang, Z., Li, Y., Chen, T., Zhang, D., Sun, F., Wei, Q., et al. (2015). Ground-level Ozone in Urban Beijing over a 1-year Period: Temporal Variations and Relationship to Atmospheric Oxidation. *Atmos. Res.* 164–165, 110–117. doi:10.1016/j.atmosres.2015.05.005
- Wang, Z., Lv, J., Tan, Y., Guo, M., Gu, Y., Xu, S., et al. (2019). Temporospatial Variations and Spearman Correlation Analysis of Ozone Concentrations to Nitrogen Dioxide, Sulfur Dioxide, Particulate Matters and Carbon Monoxide in Ambient Air, China. *Atmos. Pollut. Res.* 10 (4), 1203–1210. [In Chinese]. doi:10.1016/j.apr.2019.02.003
- Wang, Z. S., Li, Y. T., Chen, T., Zhang, D. W., Sun, F., Sun, R. W., et al. (2014). Temporal and Spatial Distribution Characteristics of Ozone in Beijing. *Huan Jing Ke Xue* 35 (12), 4446–4453. [In Chinese]. doi:10.13227/j.hj.kx.2014.12.005
- Xu, J. L., and Zhu, Y. X. (1994). Effects of the Meteorological Factors on the Ozone Pollution Near the Ground. *J. Chin. J. Atmos. Sci.* 18 (6), 751–757.
- Yang, G., Liu, Y., and Li, X. (2020). Spatiotemporal Distribution of Ground-Level Ozone in China at a City Level. *Sci. Rep.* 10 (1), 7229. doi:10.1038/s41598-020-64111-3
- Yuan, X., Feng, Z., Liu, S., Shang, B., Li, P., Xu, Y., et al. (2017). Concentration- and Flux-Based Dose-Responses of Isoprene Emission from Poplar Leaves and Plants Exposed to an Ozone Concentration Gradient. *Plant Cell Environ.* 40 (9), 1960–1971. doi:10.1111/pce.13007
- Zaveri, R. A., Berkowitz, C. M., Kleinman, L. I., Springston, S. R., Doskey, P. V., Lonneman, W. A., et al. (2003). Ozone Production Efficiency and NO<sub>x</sub>depletion in an Urban Plume: Interpretation of Field Observations and Implications for Evaluating O<sub>3</sub>-NO<sub>x</sub>-VOC Sensitivity. *J. Geophys. Res.* 108 (D14), 4436. doi:10.1029/2002JD003144
- Zhang, H. X., Sun, X., Yao, Y. H., Wan, W. X., Xiao, Y., Sun, B. F., et al. (2014). Ground-level Ozone Distribution Pattern in Summer of Beijing and its Foliar Injury Effect upon Plants. *Acta Ecologica Sinica* 34 (16), 4756–4765. doi:10.5846/stxb201306261781
- Zhang, Q. Q., and Zhang, X. Y. (2019). Ozone Spatial-Temporal Distribution and Trend over China since 2013: Insight from Satellite and Surface Observation. *Huan Jing Ke Xue* 40 (3), 1132–1142. doi:10.13227/j.hj.kx.201808028
- Zhao, S., Yin, D., Yu, Y., Kang, S., Qin, D., and Dong, L. (2020). PM<sub>2.5</sub> and O<sub>3</sub> Pollution during 2015–2019 over 367 Chinese Cities: Spatiotemporal Variations, Meteorological and Topographical Impacts. *Environ. Pollut.* 264, 114694. doi:10.1016/j.envpol.2020.114694
- Zhao, W., Gao, B., Liu, M., Lu, Q., Ma, S. X., Sun, J. R., et al. (2019). Impact of Meteorological Factors on the Ozone Pollution in Hong Kong. *Huan Jing Ke Xue* 40 (1), 55–66. [In Chinese]. doi:10.13227/j.hj.kx.201803151

**Conflict of Interest:** The authors declare that the research was conducted in the absence of any commercial or financial relationships that could be construed as a potential conflict of interest.

Copyright © 2021 Xie, Shi, Wu and Zhang. This is an open-access article distributed under the terms of the Creative Commons Attribution License (CC BY). The use, distribution or reproduction in other forums is permitted, provided the original author(s) and the copyright owner(s) are credited and that the original publication in this journal is cited, in accordance with accepted academic practice. No use, distribution or reproduction is permitted which does not comply with these terms.